Fatigue Design of Welded Aluminum Structures

CRAIG C. MENZEMER AND JOHN W. FISHER

Welded structures subjected to repeated loads often exhibit stable crack growth or fatigue. Fatigue cracking has not been limited to a single class of material or application. Reasons for these failures are numerous but in general may be linked to some shortcoming in the design process. Despite the long history associated with welded aluminum structures, comprehensive fatigue design specifications did not appear in a U.S. code until 1986. Experimental results used in the development of this specification are based primarily on fatigue tests of small specimens. Limitations on the application of such data to large structures have been documented for steel. This specification is further constrained by the lack of provisions governing variable amplitude loadings. A study was undertaken in 1988 to examine some of the issues associated with the design of welded aluminum structures. Experimentation included material characterization aimed at the development of predictive models, residual stress measurements, fatigue testing of axial specimens and beams, and detailed examination of fracture surfaces. Results pertinent to the development of the next generation fatigue design provisions are examined.

Welded structures subjected to repeated loads often exhibit subcritical crack growth or fatigue. Given the proper root conditions, crack growth normally occurs along the weld toe adjacent to the fusion line or through the weld throat. Details that fail from internal flaws, such as porosity, usually possess higher fatigue strengths as there is no geometric condition worse than the discontinuity itself (*1*). Joints with failure initiating from the weld toes require lower design stresses because the detail geometry results in large stress concentrations. Detail categories are essentially a geometric ranking of the severity of the stress concentration condition of the various joint types.

Field experience has shown that fatigue cracking is not limited to specific types of applications or to individual classes of materials. Reasons for the failures often may be attributed to inadequacies in the design process. Examples include an inadequate data and knowledge base for design provisions, cursory treatment of member interaction and joint behavior, improper detail classification, and poor definition of controlling load cases (*2,3*). This is by no means an all-inclusive list, but it does point to some of the deficiencies in current specifications.

Welded aluminum structures have been designed and built for more than 40 years. Examples include bridges, sign and luminary structures, railings, automotive and truck frames and components, cryogenic storage tanks, and so forth (*4*). Despite the application history, fatigue design provisions did not appear in a governing U.S. aluminum specification until 1986 (*5*). Most of the experimental results incorporated into the code are based on small specimen tests (*6–8*). Fatigue tests of any welded member or component should be consistent with the geometric, mechanical, and service conditions of the intended application. Any general fatigue design provisions then should reflect the lower-bound behavior of the various classes of joints. Limitations on small-scale specimens have been well documented for the case of steel structures (*9,10*). As the volume or size of the test specimen increases, the fatigue resistance decreases. Such behavior may be attributed in part to residual stresses and in part to the distribution of initial discontinuities. Simply stated, the larger the test specimen, the greater the constraint to expansion and contraction during welding. As a result, residual stresses in full-scale test samples are greater than those in smaller specimens. A decrease in fatigue strength normally accompanies an increase in the residual stresses.

All welded joints contain defects (*11–13*). Typical discontinuities include porosity, undercut, lack of fusion, large-grain structures, nonmetallic inclusions, and solidification cracks. The origin of fatigue cracks may be traced to such discontinuities. In fact, much of the fatigue resistance is consumed in the early stages of subcritical crack growth, when the defect develops into a macrocrack. As the size of the test sample increases, the probability of finding larger, more dominant flaws increases. A larger initial discontinuity will lead to a shorter fatigue life. Characterization of such discontinuity distributions allows fracture mechanics to be used to "predict" the lives of welded members and components.

COMPARISON OF ALUMINUM FATIGUE DESIGN CODES

Recent comparisons of worldwide provisions for fatigue design for aluminum structures revealed significant discrepancies in philosophy and strength values (*14,15*). Among the codes considered were the Italian or UNI 8634 (1985) specification, a draft of the British BS 8118 document (1985), the Canadian Standards Association code or the Alcan specification (1983), the 1986 version of the Aluminum Association (AA) code, and the European ECCS (1991) design provisions. Philosophical differences among these documents allow the classification of specifications into two broad groups. The Italian UNI 8634, the Canadian Standards Association, and to a limited degree the ECCS specification consider the fatigue strength to be a function of the loading, or R, ratio. R-ratio is the minimum stress in a load cycle divided by the maximum

C. C. Menzemer, Alcoa Technical Center, 100 Technical Drive, Alcoa Center, Pa. 15069. J. W. Fisher, ATLSS Research Center, 117 ATLSS Drive, Building H, Lehigh University, Bethlehem, Pa. 18015.

stress in the cycle. Both the AA and the British BS 8118 design provisions assume an R-ratio independence.

Inherent in the assumption of R-ratio independence is the influence of tensile residual stresses. Much of the fatigue life of a welded structure is spent in the formation and growth of small cracks. As a result of the tensile residual stress fields, a relatively large portion of the structure's life is spent under high mean stress levels. Even under reversed loading, the material near the initial discontinuity will be subject to a fully effective stress cycle. This is the primary justification for use of stress range as the variable that describes the fatigue resistance of welded details. Full-scale details in steel have had measurements confirming residual stresses as high as the parent material yield point (*16*). Although the presence of large tensile residual stresses has been confirmed for aluminum as well, some localized softening may prevent the stresses from approaching the base metal yield point (*17*). This, combined with tests of small-scale specimens, has given rise to the R-ratio effect. It is interesting to note that the most comprehensive specification, the ECCS document, considers fatigue strength a function of stress range. However, for cases in which the residual stresses are known, a fatigue-enhancement factor may be applied to the strength when the applied R-ratio is less than -0.25. Given the complexity of quantifying residual stresses under laboratory conditions, it seems unlikely that designers will be able to take advantage of the enhancement factor.

Variable amplitude fatigue damage is accounted for through the use of Miner's rule, with the exception of the 1986 version of the AA specification. This code gives no guidance to design or assessment of details subjected to a variable stress history. S-N curves for the British BS8118, ECCS, and newly proposed Canadian Standard employ a dual slope. Beyond the constant amplitude fatigue limit, the curves are given a second slope that implies that damage accumulates at a different rate for relatively low applied stresses. The particular value of the second slope varies between specifications, but the shapes of the S-N curves reflect the multifaceted crack-propagation behavior of aluminum.

PROJECT SCOPE AND OBJECTIVES

Early in 1988 a cooperative project was developed between the ATLSS Engineering Research Center at Lehigh University and Alcoa Laboratories. Objectives of this study included the extension of the full-scale fatigue data base for aluminum structures, examination of the behavior differences between small axial test specimens and full-scale beams, investigation of life prediction techniques, and recommendation of design rules. In support of these goals, tensile, smooth S-N fatigue, strain control fatigue, fatigue crack growth, and fracture toughness tests were conducted. Component testing included axial fatigue of plate specimens with cover plates (Figure 1)

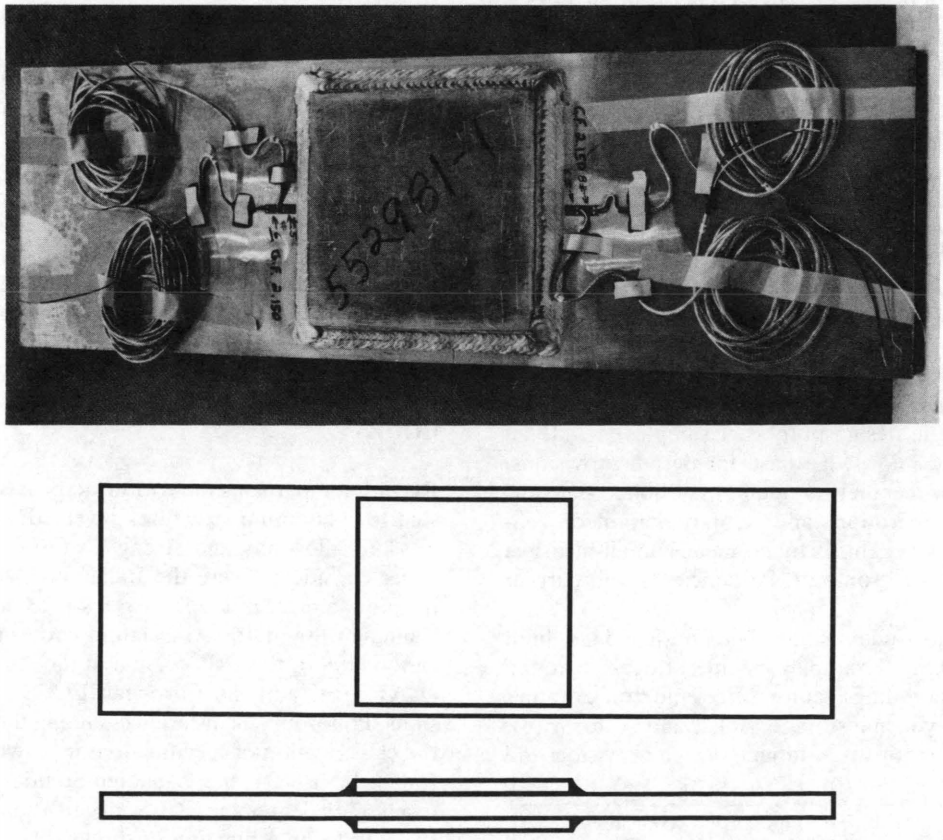

FIGURE 1 Axial cover-plate specimen: *top*, photograph; *bottom*, schematic.

and unloaded fillet-welded attachments (Figure 2). Axial cover-plate details were fabricated one at a time, while the cruciform specimens were fabricated from large welded panels that were subsequently saw-cut. Beam details tested were cover plates, stiffeners, butt-weld splices, and web-to-flange fillet welds as shown in Figure 3. Scanning electron microscopy (SEM) examinations of fracture surfaces were used to establish failure locations, defect sizes, orientations, and mechanistic differences in crack propagation under controlled environmental conditions.

Fatigue life prediction traditionally has used both fracture mechanics and strain control methodologies. Both techniques were explored for the constant amplitude behavior of the cover plate and stiffener beam details. Predicted S-N curves were compared to the experimental results as a means of assessing their applicability to full-scale welded aluminum details. Variable amplitude behavior was examined through extension of the fracture mechanics model. Several stress spectrums were chosen to yield applicable stress range values and included constant, linear, and Rayleigh distributions.

As the amount of work conducted in this study is beyond the present scope, emphasis will be placed on results that directly address design issues. The specifics of the residual stress measurements have been discussed elsewhere, so only the conclusions will be reviewed (*18*). Toughness of weldable aluminum alloys has been an issue that has, on occasion,

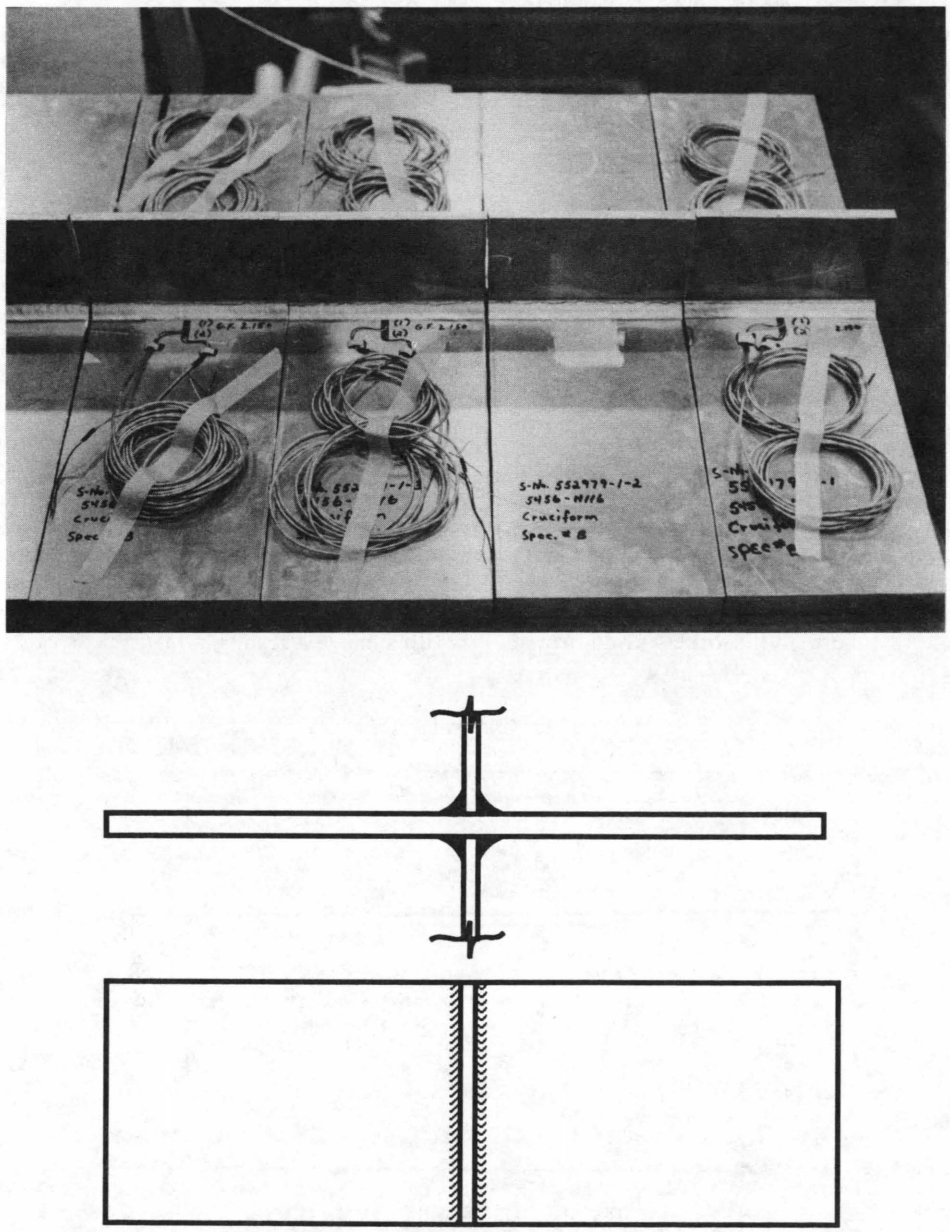

FIGURE 2 Cruciform joint: *top*, photograph of cruciform joints cut from plate; *bottom*, schematic of cruciform joint test specimens.

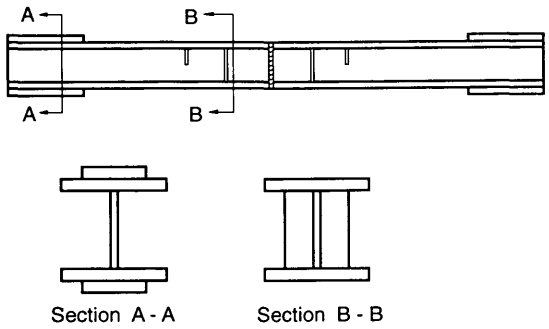

FIGURE 3 Elevation of full-scale beam sample, showing details of two sections.

restricted applications. *R*-curve tests of 5456-H116 and A36 steel will be discussed. Component fatigue tests and the impact on current design specifications will be examined. A brief discussion of the variable amplitude modeling and its impact on the code will follow.

RESIDUAL STRESS MEASUREMENTS

The existence of residual stresses in welded components significantly influences the fatigue behavior of the components. During the course of this study, residual stresses were measured on as-fabricated beams and axial fatigue specimens. In addition, measurements were taken on samples that had been tested but that contained no evidence of fatigue damage. In all cases, the hole-drilling technique was used (*19*).

Residual stress measurements demonstrated that significant differences exist between full-scale and small axial specimens. Maximum residual stresses for the cruciform panel and cover-plated beam details typically reached 80 degrees of the parent metal yield strength. The axial test samples, on the other hand, typically had residual stresses of 40 to 50 percent of the parent metal strengths. Figure 4 illustrates as-fabricated residual stresses for a cruciform panel and axial specimens cut from the panel. Such differences may be attributed to constraint developed around the detail during welding. Measurement comparisons on as-fabricated and tested details showed no appreciable change of the surface residual stresses as a result of elastic cyclic loading. As much of the fatigue resistance is consumed in the growth of small defects, it is reasonable to conclude that the residual stresses have a major impact on the behavior of welded aluminum structures. In addition, residual stresses of this magnitude are consistent with fatigue failures observed on the compression side of the beams.

FRACTURE TOUGHNESS

Material toughness is often a secondary consideration in the minimization of cracking. Of primary importance is the design and selection of fatigue-resistant details and quality assurance in the shop during fabrication. Over the past three decades, a number of localized failures have developed in welded structures as a result of fatigue crack growth. In a few cases, subcritical crack growth eventually led to failure of the structure by rapid fracture. Most of these failures could not have been prevented by increased material toughness alone (*20*). However, some such failures have had catastrophic consequences; as a result, emphasis has been placed on forgiving materials and measurement of the appropriate properties.

Toughness of many of the structural aluminum alloys cannot be characterized by any of the currently available standardized test methods (*21*). Given the difficulties in crack tip characterization when the plastic zone is large, a comparison of the fracture behavior of 5456-H116 and A36 steel was undertaken nevertheless. As none of simple screening tests are considered applicable to both aluminum and steel, compact tension samples and *R*-curve testing seemed most suitable. A schematic of a compact tension specimen is shown with some test results in Figure 5. Loads are applied through

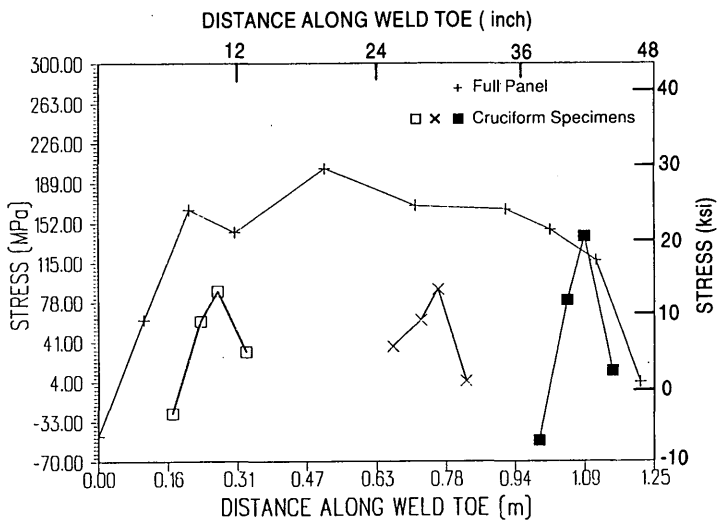

FIGURE 4 Residual stress profile for cruciform panels and fabrication axial specimens.

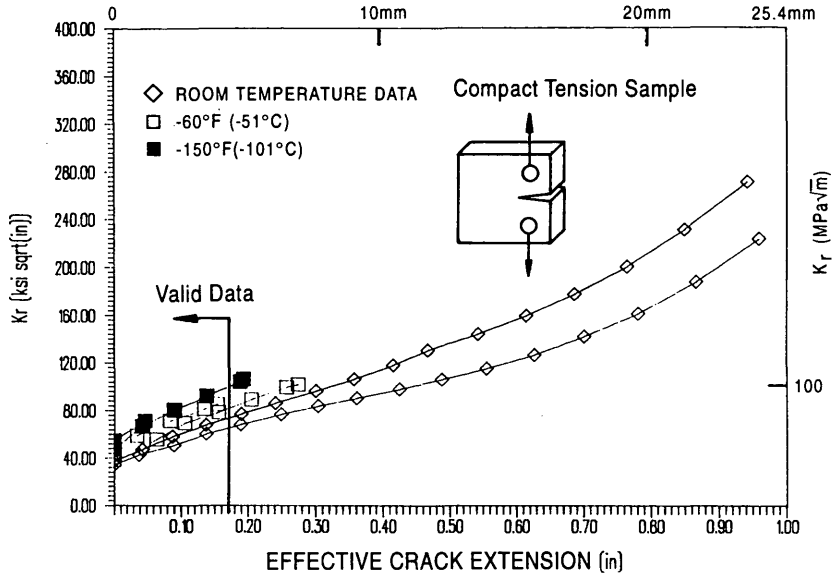

FIGURE 5 Curves for A36 steel specimens tested at +75°F and −150°F.

pins placed in the holes. Because the ductility of both materials would result in prohibitively large specimen dimensions not representative of practical applications, specimens were chosen to be 1.0 in. thick. Tests were conducted at room temperature, −60°F, −150°F, and −200°F. The −60°F toughness requirements are typical of many structural specifications (*22*).

An *R*-curve is a plot of a material's resistance as a function of effective crack extension. Material resistance may be defined by the stress intensity factor, K_r. From a practical standpoint, K_r is a measure of the magnitude of the stress field around the crack tip. Effective crack extension comprises the physical crack length and the plastic zone correction. Around the tip of a crack is a region where the material is plastically deformed. The presence of such a region makes the crack behave as if it were slightly larger than the physical crack size itself. Crack extension implies that the increment of crack growth is plotted as the ordinate of the *R* curve.

Figure 5 summarizes the test results for the A36 steel samples over the range of temperatures considered. Room temperature data indicate the development of large toughness values throughout the range of crack growth. Behavior at −60°F and at −150°F is markedly different. Both of these data sets show a reduction in the material's resistance to crack extension. What is more striking is the reduction in amount of stable crack extension before failure. Comparison of fracture surfaces also showed a decrease in shear lip development and specimen thinning as the test temperature was lowered. Smaller amounts of plastic deformation indicate a drop in toughness.

Figure 6 summarizes the aluminum test results for the range of temperatures considered. Room temperature response shows

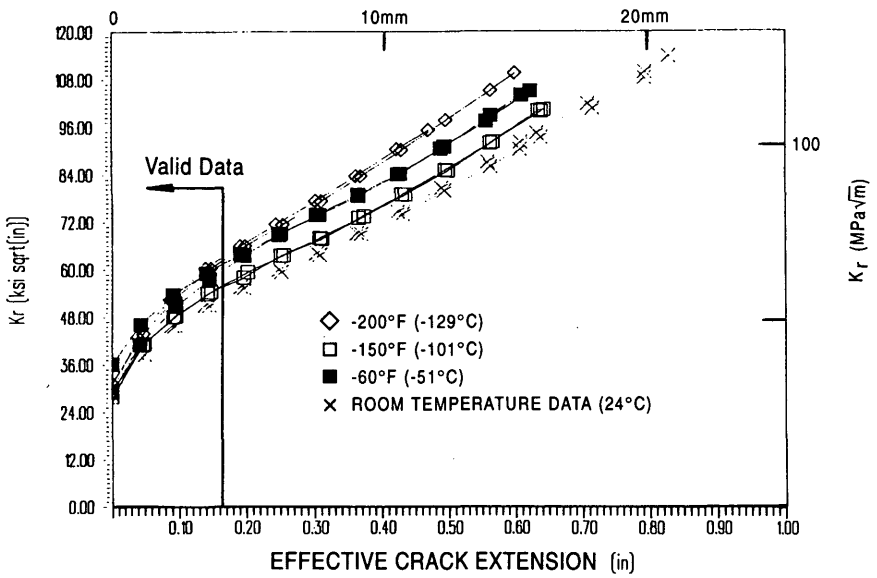

FIGURE 6 Aluminum specimen *R*-curves for the range of temperatures.

a rising R-curve throughout the range of stable crack extension. Behavior at the lower temperatures is not significantly different. Although the amount of stable crack extension is somewhat smaller, the difference is less than that observed for the A36 steel. Maximum toughness values increase with a decrease in temperature. Further, all specimens tested showed evidence of plastic deformation, even at the lowest temperature considered.

Both sets of curves show a slight reversal in curvature near the center of the plots. This is indicative of specimens too small to obtain valid, linear elastic test results. Implicit in the calculation of K_r is the assumption of small-scale yielding. Materials with significant ductility are difficult to characterize with any of the currently available techniques. As such, the vertical lines in Figures 5 and 6 indicate the range of valid data. Further, the elevation of toughness with decreasing temperature is consistent with the increase in yield point at lower temperatures. As the temperature is decreased, an equivalent crack opening displacement will require an increase in the load. This will correspond to an increase in the stress intensity factor.

A comparison between aluminum and steel R-curves by like temperature conditions reveals several interesting trends. At room temperature, the A36 exhibits larger resistance values over the entire range of stable crack extension. At the lower temperatures, the aluminum samples developed toughness equal to or greater than the A36. Also, the 5456-H116 specimens show a wider range of stable crack extension before failure.

A36 steel has been successfully used in welded structures for many years. Given the difference in modulus values and crack propagation rates, a similar aluminum structure will have dimensions somewhat larger and be designed for lower allowable stresses. As a result, a direct comparison of toughness should be made on resistance values normalized to reflect this difference. Figure 7 compares room temperature R curves that have been normalized with an effective driving force. Category C constant amplitude fatigue limits of 10 and 4 ksi were used as the applied stress ranges for the steel and aluminum samples respectively. Crack lengths were taken to be those measured in the tests. In the context of allowable fatigue design provisions, the 5456-H116 alloy shows larger resistances to crack extension. The same trend is apparent at lower temperatures as well.

Fatigue tests on full-scale welded beams further demonstrated the ability of 5456-H116 to resist and arrest unstable crack extension under realistic loading conditions. In no case was there rapid fracture that completely severed a beam.

COMPONENT FATIGUE TESTS

Twelve beams were tested in four-point bending. This allowed evaluation of 48 cover-plate details, 96 stiffeners, and 24 butt splices. Tests were conducted using closed-loop servohydraulics with digital control. To accompany the beams, 32 axial tests on cover plates and cruciform joints were completed. All plate thicknesses and weld dimensions were the same on the axial and beam samples to minimize any "thickness" effect. Fatigue cracks on the beams were allowed to grow through the plate thickness; then the damage was repaired by splicing, drilling stop holes, or both. Tests were resumed until failure occurred at another location.

Figure 8 compares the performance of the axial cruciforms and beam stiffener samples. Also shown is the mean regression line for each. As is easily seen, there is a significant difference in the mean resistance of the two sample types. The difference appears to increase with the number of applied cycles. Figure 9 compares the results of the beam tests with the current AA Category C design curve. It should be noted that the specification provides fatigue strengths in tabular form although the continuous curve is shown here. Category

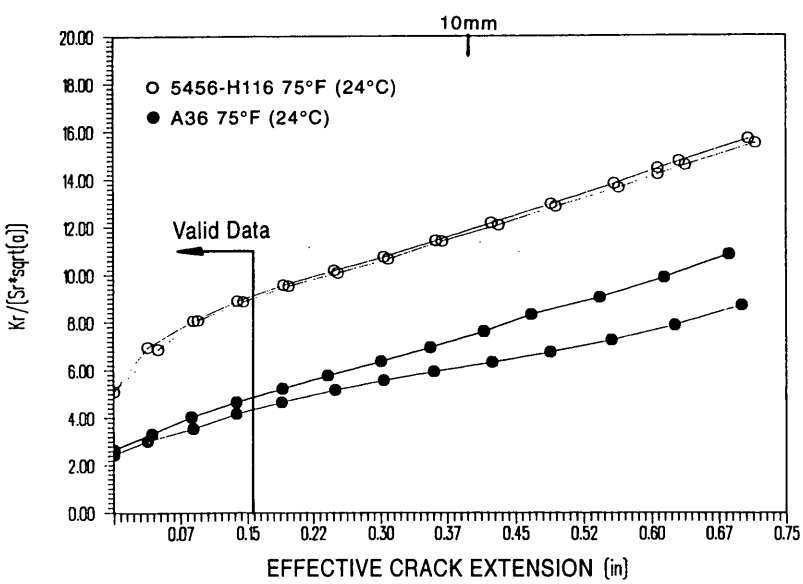

FIGURE 7 Room-temperature comparison of normalized R-curves using Category C.

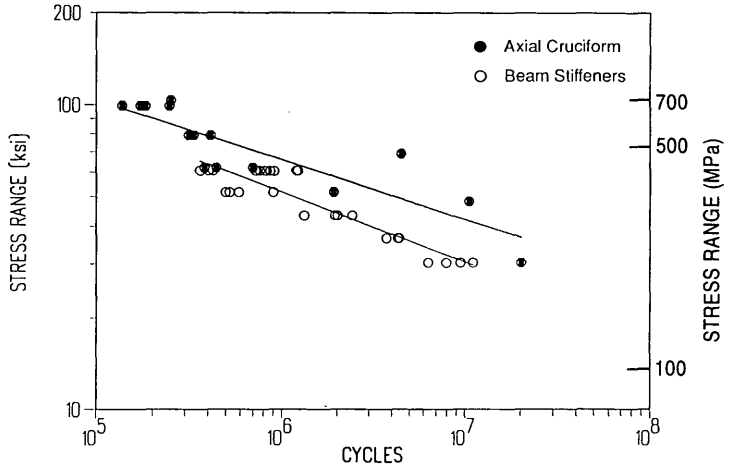

FIGURE 8 Comparison of stiffener details and axial joints with mean regression lines.

C is slightly unconservative as compared with the test results. Several of the points plot on or below the design curve.

The axial cover plate and beam detail test results were compared. Regression analysis used to develop the 95 percent confidence limits for 97.5 percent probability of survival showed a significant difference in the lower-bound fatigue resistance. As expected, the limit for the beam samples is lower than for the axial samples. Figure 10 compares the beam cover-plate data with Category E of the 1986 AA specification. The design category appears to be somewhat conservative. The band of the data appears to be rotated upward as compared with the design curve. Increasing the design strengths may be warranted but will require review of other full-scale data above 2×10^6 cycles.

VARIABLE AMPLITUDE BEHAVIOR MODEL

A fracture mechanics model was developed for the constant amplitude case and verified through comparison with the beam data. This model was then extended to the case of variable amplitude loadings. Specifics of the model have been discussed elsewhere, and only a review pertinent to assessment and design is presented here.

Stress intensity factors were developed from well-known handbook solutions (*23*). Crack-growth information for a 5XXX series alloy was taken from a compendium of curves and was based on the K_{max}, ΔK decreasing test procedure (*24*). Such information is thought to be representative of crack growth in welded structures as closure is diminished. Several shapes of loading spectrums were considered including constant, linear, and Rayleigh distributions. Either the spectrums were shifted or smaller stress cycles were truncated to obtain different characteristic stress range levels. Overloads were applied at different frequencies. An overload is a stress cycle that exceeded the constant amplitude limit. Emphasis was on examining cover-plate details.

Several methods were used to define an equivalent characteristic stress for the distributions. These included a fourth-order transformation of Miner's rule and an equivalent con-

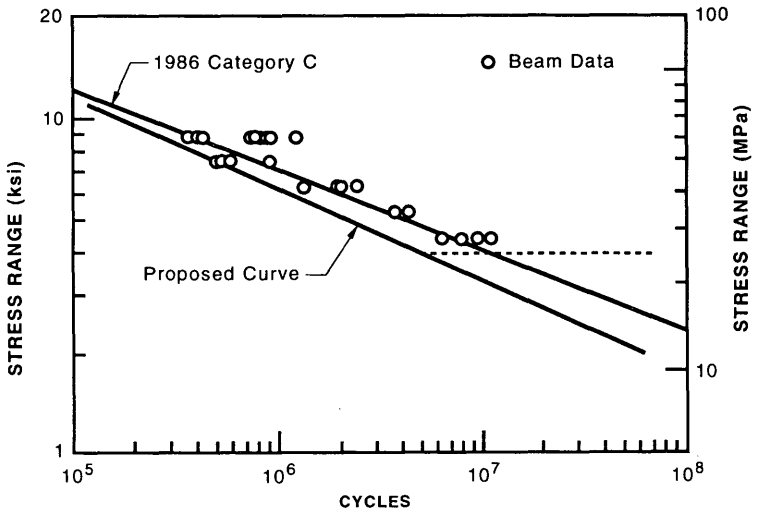

FIGURE 9 Comparison of stiffener test data with current specification Category C and proposed design curve.

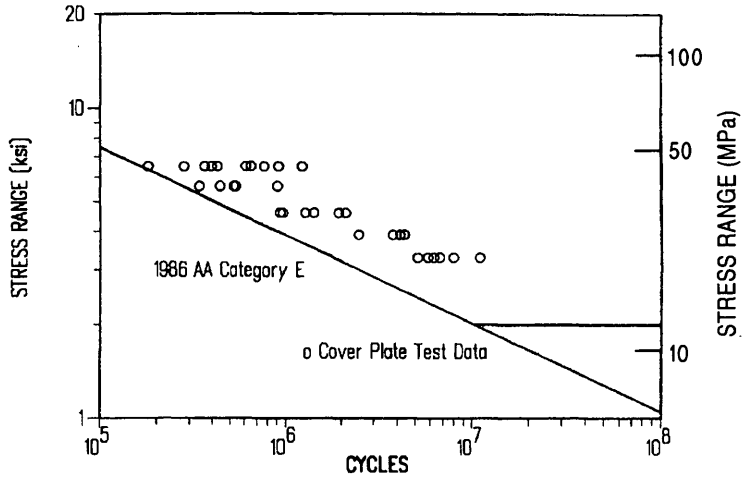

FIGURE 10 Cover-plate data compared with 1986 version AA Code Category E.

stant amplitude stress range that resulted in the same amount of damage. Miner's rule may be given by

$$\sum \left(\frac{n}{N}\right) = 1 \tag{1}$$

where n is the number of cycles applied at a specific stress range and N is the number of cycles to failure at that stress range. Assuming a straight-line S-N relationship, Miner's rule may be transformed to

$$S_{rc} = \left(\sum \alpha_i S_{ri}^b\right)^{1/b} \tag{2}$$

where

α_i = frequency of occurrence of ith stress range,
S_{ri} = ith stress range in spectrum,
b = slope of S-N curve, and
S_{rc} = characteristic stress range for distribution.

For Miner's rule, both nominal stress ranges and effective stress ranges were calculated. Nominal values include all the stress cycles in the spectrum, whereas effective stress ranges include only those cycles contributing to crack growth. General trends in the behavior were the same, regardless of the stress range definition employed.

Figure 11 illustrates the predicted response of the cover plate to a linear stress spectrum shift with overload frequencies varying from 0 to 0.1 percent. Crack growth occurred even though the nominal stress range is below the constant amplitude fatigue limit. The outermost point had a characteristic stress range of 1.7 ksi and a maximum stress in the spectrum only slightly above the fatigue limit of 3 ksi. Overloads of 1.0 ksi plus the maximum stress in the spectrum were considered as well. As the frequency of this overload in-

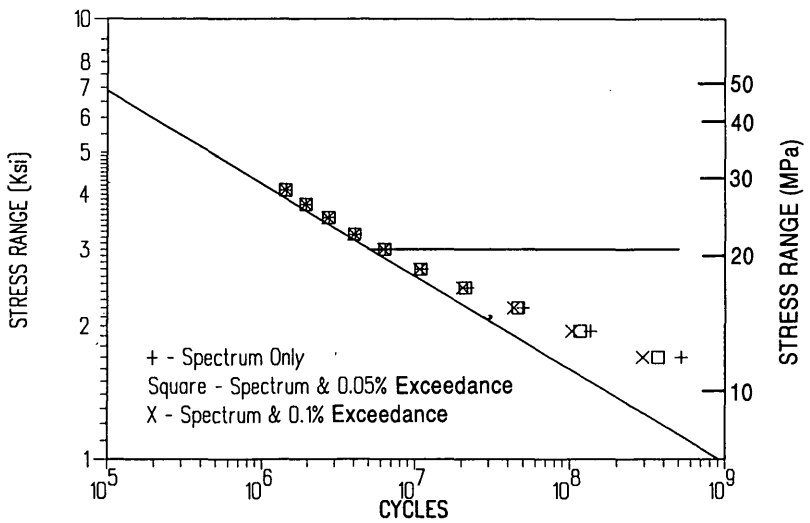

FIGURE 11 Influence of overload on the fatigue resistance of cover plates—linear spectrum.

creases, the S-N curve is pulled downward or the resistance is decreased. This is most pronounced for lives greater than 10^7 cycles. As the number of cycles in the spectrum exceeding the constant amplitude fatigue limit increases, there is little if any influence of the overload.

Figure 12 illustrates cover-plate response to a linear spectrum shift with no overloads but with all three definitions of the characteristic stress. Each curve shows the same general shape, and the difference between the stress ranges at any given life is less than 0.6 ksi. This difference is largest at the lowest stresses considered but becomes significantly smaller as the number of cycles exceeding the fatigue limit increases. In addition, it seems unlikely that stresses can be calculated or measured within a 0.6 ksi spread; so many of the arguments as to which stress definition is correct are of theoretical importance only. This is to be expected, because most cycles in the spectrum contribute to growth when the characteristic stress approaches the fatigue limit. It is interesting to note that the equivalent constant amplitude stress range falls between the bounds as defined by Miner's rule.

SUMMARY

Residual stress measurements confirmed the existence of large tensile residual stresses in full-scale welded aluminum components. Peak stresses were on the order of 80 percent of the parent metal yield strength, but the axial specimens showed maximum values closer to 40 or 50 percent. Measurements on tested, but undamaged, specimens showed that shakedown was minimal and that the residual stresses are present for a significant portion of the fatigue life. For general-purpose design specifications, stress range is the appropriate strength variable and any enhancement at full reversal should not be taken advantage of.

Fracture toughness tests on 5456-H116 illustrated the ability of the material to deform plastically in the presence of a notch at temperatures down to −200°F. Comparisons with A36 steel revealed that in the context of allowable fatigue design provisions, the aluminum alloy gave a higher degree of damage tolerance and toughness. Fatigue tests on the beams confirmed the ability of the material to arrest cracks before complete member separation. A36 has been used successfully in welded structures for many years, so a properly designed aluminum structure should give adequate performance.

Component fatigue tests showed that in general, the details on the beams defined the lower bound on fatigue resistance compared to the flat-plate specimens. Current aluminum specifications are slightly overconservative for Category C joints; some adjustment in the Category C allowable design stresses is warranted. Cover-plate beam details did not follow current design provisions. Further long-life data review is warranted before Category E design constraints are relaxed.

An extension of the fracture mechanics model demonstrated that crack growth could occur when the characteristic stress was below the fatigue limit. Furthermore, it seems likely that variable amplitude behavior may be assessed using constant amplitude design data and a fourth-order representation Miner's rule. Comparisons of different characteristic stress definitions showed that the differences were small and were largely of academic interest.

Overloads had the greatest influence on the variable amplitude response when the number of cycles exceeding the fatigue limit was small. As the frequency and magnitude of the overload increased, the high cycle portion of the S-N curve was pulled downward. The result was a reduction in fatigue resistance. When exceedance levels became large, the overload appeared to have no influence on the cover plate behavior. A lack of variable amplitude data makes further recommendations difficult. Additional data are needed for comparison to the models and for further development of design guidelines.

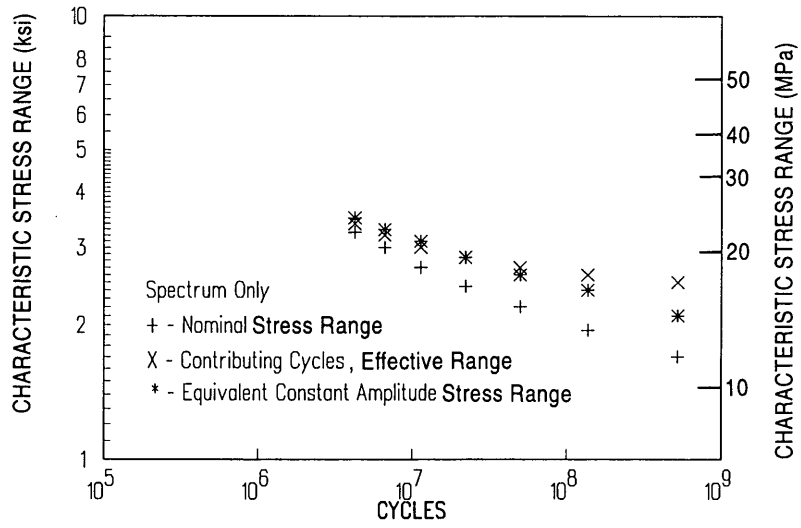

FIGURE 12 Comparison of effective stress range defined by Miner's rule or by crack-growth model.

REFERENCES

1. J. W. Fisher. *Bridge Fatigue-Guide—Design and Details*. American Institute of Steel Construction, Chicago, Ill., 1977.
2. J. W. Fisher and C. Demers. *A Survey of Localized Cracking in Steel Bridges 1981–1988*. ATLSS Report 89-01. Lehigh University, Bethlehem, Pa., 1989.
3. J. W. Fisher and C. Menzemer. *Case Studies and Repair of Fatigue Damaged Structures, Structures Subjected to Repeated Loading*. Stability and Strength Series, No. 9, Elsevier, New York, N.Y., 1990, Chapter 7.
4. *Welding Alcoa Aluminum*. Aluminum Company of America, Pittsburgh, Pa., 1972.
5. *Specifications for Aluminum Structures*. Aluminum Association, Washington, D.C., 1986.
6. W. W. Sanders. *Fatigue Behavior of Aluminum Weldments*. Bulletin 171. Welding Research Council, New York, N.Y., April 1972.
7. W. W. Sanders and R. H. Day. *Fatigue Behavior of Aluminum Alloy Weldments*. Bulletin 286, Welding Research Council, New York, N.Y., Aug. 1983.
8. W. W. Sanders and J. W. Fisher. *Recommended Specifications for Fatigue Design of Aluminum Structures*. Submitted to the Aluminum Association, Washington, D.C., 1985.
9. P. B. Keating and J. W. Fisher. *NCHRP Report 286: Evaluation of Fatigue Tests and Design Criteria on Welded Details*. TRB, National Research Council, Washington, D.C., 1986.
10. D. Kosteas. Fatigue Design—Background, Assumptions, and Practical Concepts. *Proc., 8th International Light Metals Congress*, Vienna, Austria, 1987.
11. R. Jaccard. Fatigue Life Prediction of Aluminum Structures Based on S-N Curve Simulation. *Proc., 2nd International Conference on Aluminum Weldments*, Munich, Germany, 1982.
12. *Structural Welding Code*. American Welding Society, Miami, Fla., 1983.
13. J. Barsom and S. T. Rolfe. *Fracture and Fatigue Control in Structures, Applications of Fracture Mechanics*, 2nd ed. Prentice Hall, Englewood Cliffs, N.J., 1987.
14. A. Mandra, F. M. Mazzolani, and E. Mele. Fatigue of Aluminum Alloy Joints—Comparison of Codification. *Proc., 5th International Aluminum Conference*, Munich, Germany, 1992.
15. I. J. J. Van Straalen, F. Soetens, and O. D. Dijkstra. *Inventory and Comparison of Fatigue Design Codes for Aluminum Alloy Structures*. Report B-89-714. TNO Institute for Building Materials and Structures, Apeldoorn, The Netherlands, 1990.
16. R. Roberts et al. *Determination of Tolerable Flaw Sizes in Full-Scale Welded Bridge Details*. Report FHWA-RD-77-170. FHWA, U.S. Department of Transportation, 1977.
17. S. J. Maddox. Fatigue Design of Welded Aluminum Alloy Structures. *Proc., 2nd International Conference on Aluminum Weldments*, Munich, Germany, 1982.
18. C. Menzemer and J. W. Fisher. Fatigue Behavior of Welded Aluminum Structures. *Proc., 5th International Aluminum Conference*, Munich, Germany, 1992.
19. *Measurement of Residual Stresses by the Hole Drilling Strain Gage Method*. Technical Note 503-3. Measurements Group, Raleigh, N.C., 1988.
20. J. Barsom et al. Fracture Control Considerations for Steel Bridges. *Workshop Proceedings*. FHWA, U.S. Department of Transportation, Atlanta, Ga., 1977.
21. *The Aluminum Association Position on Fracture Toughness Requirements and Quality Control Testing*. Report T-5. Aluminum Association, Washington, D.C., 1971.
22. *Standard Specifications for Highway Bridges*, 13th ed. AASHTO, Washington, D.C., 1983.
23. H. Tada, P. Paris, and G. Irwin. *The Stress Analysis of Cracks Handbook*. Del Research Corp., Hellertown, Pa., 1973.
24. R. Jaccard. *Fatigue Crack Propagation in Aluminum*. Document XIII-1377-90. International Institute of Welding, London, England, 1990.

Publication of this paper sponsored by Committee on Steel Bridges.